Complementary Probe of a two-component Dark Matter Model with Gravitational Waves at LISA

Pankaj Borah

Department of Physics
Indian Institute of Technology Delhi

PPC 2024

14 -18 October 2024, Hyderabad, India

IITD

17th International Conference on Interconnections between Particle Physics and Cosmology

Motivation

- Among many, the two issues that the Standard Model of particle physics cannot answer:

  - Dark Matter candidate
  - The origin of Baryon Asymmetry of the Universe

Motivation for Beyond the Standard Model !

- After the Higgs Boson discovery in 2012, the detection of Gravitational Waves (GW) in 2016 is the other major discovery in our time.

  * A new window into the early Universe

Is there any connection among them ?

▪ Complementarity

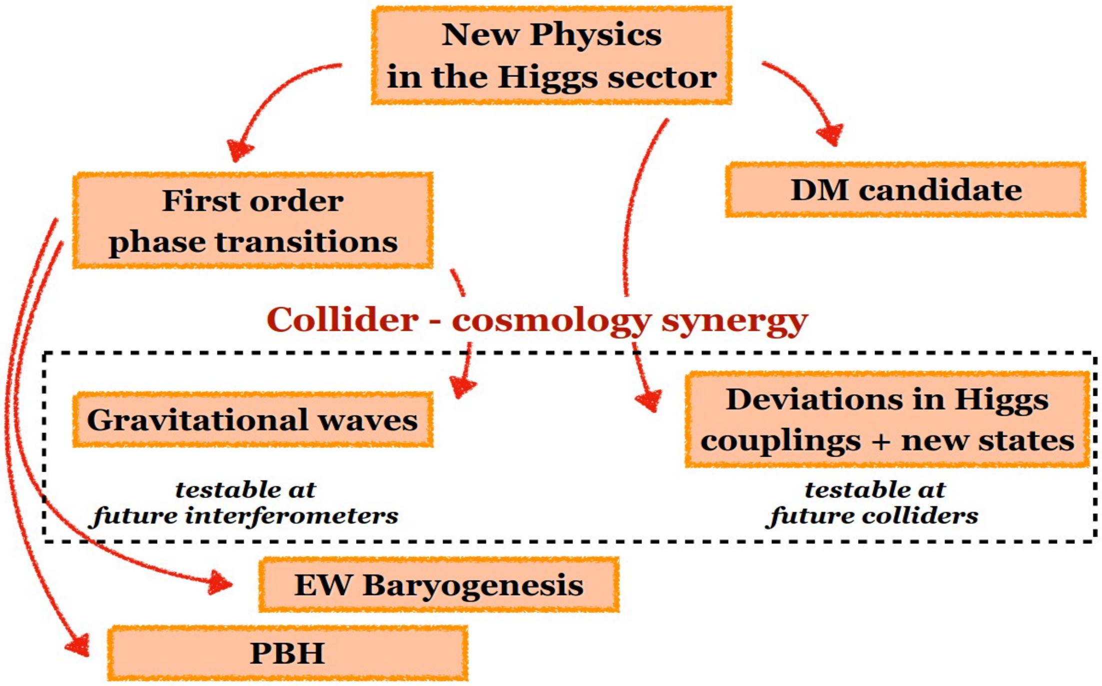

*Image: ***Luigi Delle Rose***

Gravitational Wave Observation

A complementary way to explore or discard new physics model

Cosmology with Gravitational Waves

- **GWs are a probe for Early Universe**

What process of the Early Universe source GWs?

- GWs from Inflation
- GWs from Preheating
- GWs from Phase Transitions
- GWs from Cosmic Defects

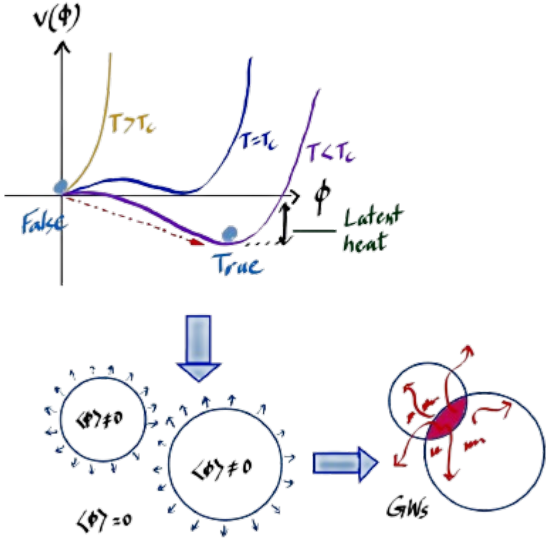

- **GWs from First-order "EW Phase Transitions"**

Prereq Check

The main production processess are,

- **Bubble collisions**
- **Sound waves left behind in thermal plasma**
- **Turbulance**

EW Baryogenesis

SM with Inert Triplet Scalar

- **First, we cosider a framework with the SM extended with *SU(2)* triplet scalar with *Y = 0*.**

$$T = \frac{1}{2}\begin{pmatrix} T_0 & \sqrt{2}T^+ \\ \sqrt{2}T^- & -T_0 \end{pmatrix}$$

In a simple set-up, imposing Z_2 symmetry can ensure the stability of T_0 and be a DM candidate.

The scalar potential is given as,

$$\boxed{V(H,T) = -\mu^2 H^\dagger H + \mu_T^2 \mathrm{Tr}(T^\dagger T) + \lambda_1 |H^\dagger H|^2 + \lambda_t (\mathrm{Tr}|T^\dagger T|)^2 + \lambda_{ht} H^\dagger H \mathrm{Tr}(T^\dagger T)}$$

- **Key findings in existent literatures,**
  - Thermal relic is satisfied for heavier DM mass, $m_{T^0} \geq 1.8\,\mathrm{TeV}$
  - DD constraints can be evaded for DM mass, $m_{T^0} \geq 1.2\,\mathrm{TeV}$

$$\sigma_{\mathrm{SI}} \propto \frac{\lambda_{ht}^2}{m_H^2 m_{T^0}^2}$$

  - An SFOPT demands the mass of the new neutral scalar state, $m_{T^0} \simeq 250\,\mathrm{GeV}$ for a max. of $\lambda_{ht} \lesssim 1.95$ *P. Bandyopadhay et al. Phys.Rev.D 107 (2023)*

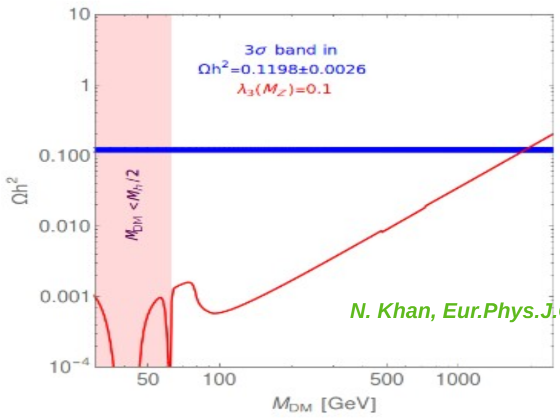

N. Khan, Eur.Phys.J.C 78 (2018)

"Tensions with DM observations and SFOPT predictions"

A multi-component DM scenario

Let's consider an extension of the Inert Triplet Scalar with a real scalar and a Dirac fermion singlet under *SU(2)*.

Objectives:

- Explore the "desert" region of the ITM DM scenario.
- Look for parameter spaces where both the criteria of an SFOPT and DM constraints can be fulfilled, provided T^0 remains in the desert region.
- Investigate the GW frontiers for complementary searches.

	S	T	ψ
$\mathcal{Z}_2$	$+1$	$+1$	-1
$\mathcal{Z}_2'$	$+1$	-1	$+1$

A $\mathcal{Z}_2 \times \mathcal{Z}_2'$ is imposed, under which T^0 and ψ are DM candidates.

The extended scalar Lagrangian,

$$\mathcal{L} \equiv \mathcal{L}_{\rm SM} + \mathcal{L}_{\rm Trip} + \mathcal{L}_{\rm S} + \mathcal{L}_{\psi} + \mathcal{L}_{\rm int}$$

Scalar Singlet-Triplet with a Dirac Fermion

Let's consider an extension of the Inert Triplet Scalar with a real scalar and a Dirac fermion singlet under *SU(2)*.

Relevant potential and interaction:

$$V(H,T,S) = V(H) + V(H,T) + V(H,S) + V(S,T)$$

$$V(H) = -\mu_H^2 H^\dagger H + \lambda_H (H^\dagger H)^2$$

$$V(H,T) = -\frac{\mu_T^2}{2}\mathrm{Tr}(T^\dagger T) + \frac{\lambda_T}{4}(\mathrm{Tr}(T^\dagger T))^2 + \frac{\lambda_{HT}}{2}\mathrm{Tr}(T^\dagger T)(H^\dagger H)$$

$$V(H,S) = -\frac{\mu_S^2}{2}S^2 + \frac{\lambda_S}{2}S^4 + \mu_{HS}(H^\dagger H)S + \frac{\lambda_{SH}}{2}(H^\dagger H)S^2 - \frac{\mu_3}{3}S^3$$

$$V(S,T) = \frac{\mu_{ST}}{2}\mathrm{Tr}(T^\dagger T)S + \frac{\lambda_{ST}}{2}\mathrm{Tr}(T^\dagger T)S^2$$

$$\mathcal{L}_\psi = \bar{\psi}\,(i\partial - \mu_\psi)\,\psi - g_s \bar{\psi}\psi S$$

	S	T	ψ
$\mathcal{Z}_2$	$+1$	$+1$	-1
$\mathcal{Z}_2'$	$+1$	-1	$+1$

A $\mathcal{Z}_2 \times \mathcal{Z}_2'$ is imposed, under which T^0 and ψ are DM candidates.

- We consider non-zero VEV for the singlet

$$\langle S \rangle = v_s$$

- Due to non zero VEV of *S*, it mixes with *H* with mixing angle $\tan 2\theta = \frac{\lambda_{SH} v v_s}{\lambda_H v^2 - \lambda_S v_s^2}$
- **Independent parameters are:**

$$m_{T^0}, m_S, m_\psi, \mu_3, \mu_{ST}, v_s, \sin\theta, g_s, \lambda_S, \lambda_T, \lambda_{HT}, \lambda_{ST}$$

Brief comment on Parameters

Crucial parameters DM1

$$m_{T^0}, \lambda_{HT}, \lambda_{ST}$$

Crucial parameters DM2

$$m_{h_2}, m_\psi, \sin\theta, v_s, g_S$$

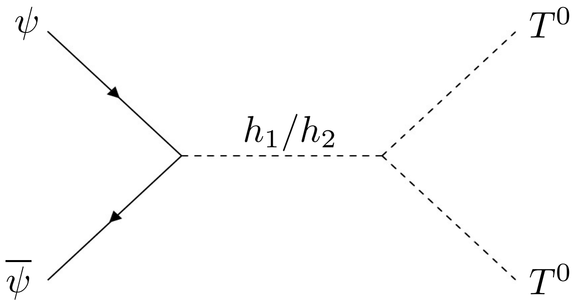

$$\lambda_{h_1 T^0 T^0} = \lambda_{HT} v \cos\theta + \mu_{ST}\sin\theta + \lambda_{ST} v_s \sin\theta$$

$$\lambda_{h_2 T^0 T^0} = -\lambda_{HT} v \sin\theta + \mu_{ST}\cos\theta + \lambda_{ST} v_s \cos\theta$$

Crucial parameters DM1 ⟷ DM2

$$g_S, \mu_{ST}$$

What we consider:

- We want Triplet DM to be under-abundant with mass below 1 TeV
- Couplings controlling DM1 abundance should be below 1

So that DM+PT remain in the same page !

General Scan and Results

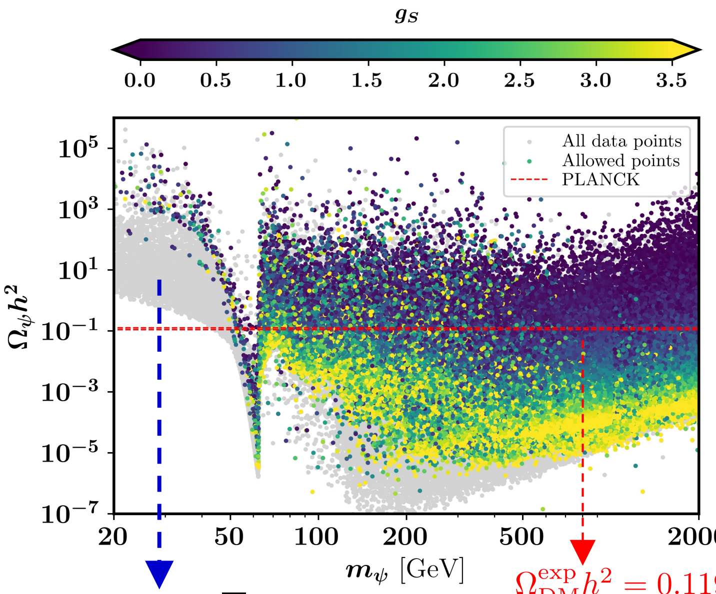

$\Omega_{\rm DM}^{\rm exp} h^2 = 0.1199 \pm 0.0027$

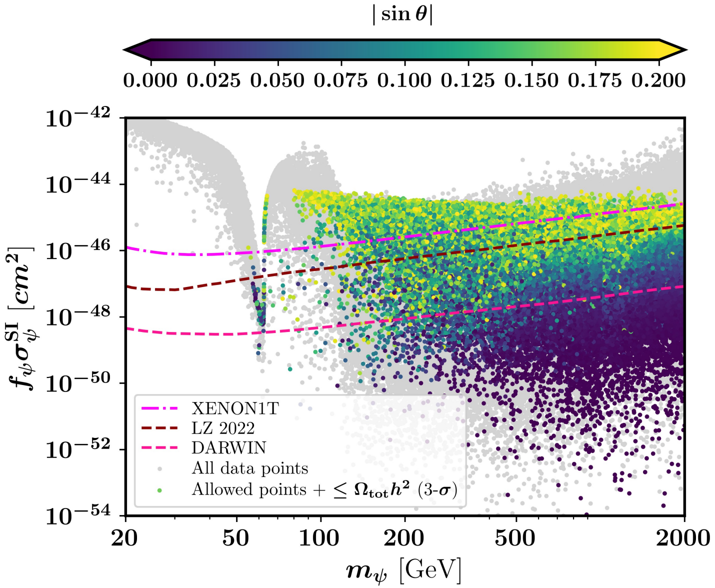

$h_1 \to \psi\overline{\psi}$

$$\Gamma(h_1 \to \psi\overline{\psi}) \simeq \frac{g_S^2 m_{h_1} \sin^2\theta}{8\pi} \left(1 - \frac{4m_\psi^2}{m_{h_1}^2}\right)^{3/2}$$

$$f_i = \frac{\Omega_i h^2}{\Omega_{\rm DM} h^2}, \quad \sigma_\psi^{\rm SI} \propto g_S^2 \sin^2(2\theta) \left(\frac{1}{m_{h_1}^2} - \frac{1}{m_{h_2}^2}\right)^2$$

- Very small values of g_S and $|\sin\theta|$, together, results in overproduction of the fermionic DM, leading to their exclusion based on DM relic constraints.
- Comparatively larger g_S underproduces ψ-DM, however it can be compensated by smaller $|\sin\theta|$.
- Smaller $|\sin\theta|$, i.e., $\mathcal{O}(10^{-2})$ or less, is favoured to avoid LZ and DARWIN limits on direct detections.

General Scan and Results

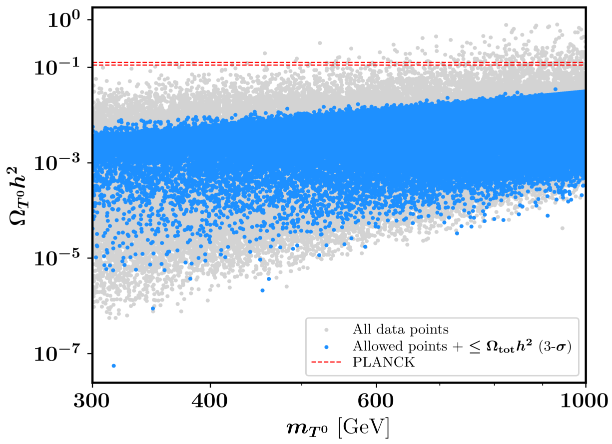

- In some cases, the triplet DM relic exceeds the PLANCK-measured relic limit. Purely due to DM-DM conversion.
- Such scenario mainly corresponds to very small $g_S\left(\mathcal{O}(10^{-2})\right)$, which is heavily challenged from DM relic constraints as it produces, in general, overabundant ψ-DM.
- In the considered phenomenologically viable region, i.e., [300, 1000] GeV, triplet DM remain underabundant.

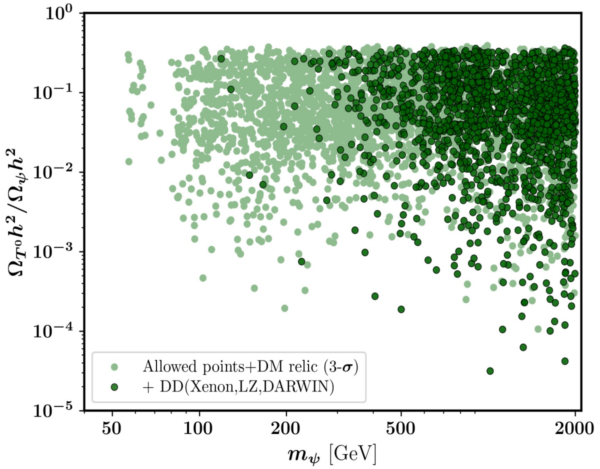

- In our model set-up, **the fermion DM is the dominant one**.
- However, due to DM-DM conversion, **there is an enhancement in contribution** to $\Omega_{\rm tot}h^2$ upto 26% for the T^0-DM, which is otherwise below 10% in a pure *Y=0* triplet DM set-up for DM mass below 1 TeV.
- In some cases, the T^0 contribution is often being suppressed by up to five orders of magnitude. This suppression is necessary for evading the exclusion limits on the T^0 SI cross-section.

General Scan and Results

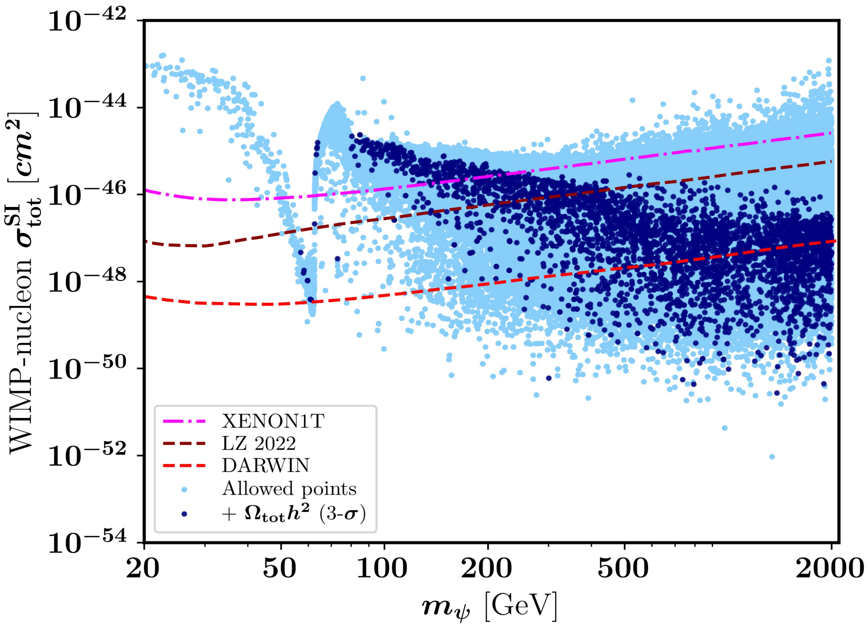

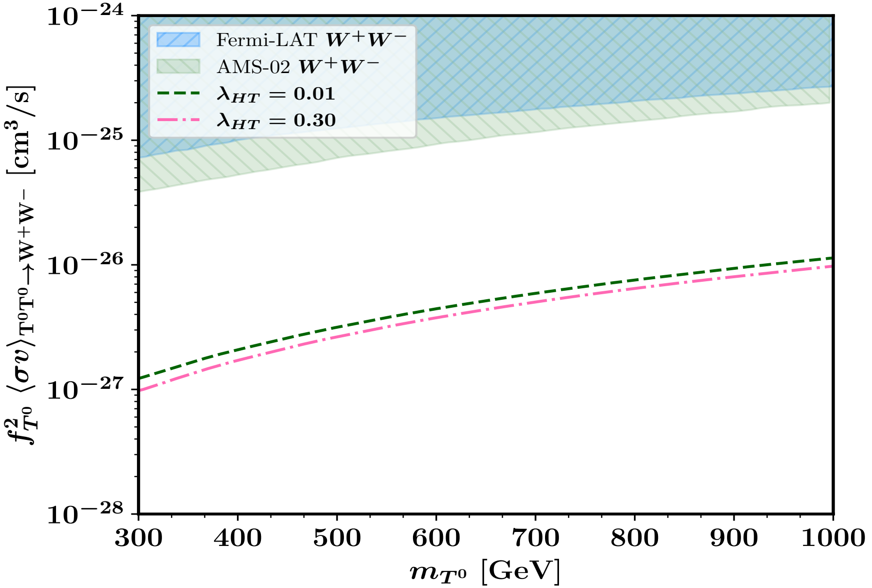

$$\frac{\sigma^{\rm SI}_{\rm exp}}{M_{\rm DM}} > \frac{f_{\rm DM1}}{M_{\rm DM1}}\,\sigma^{\rm SI}_{\rm DM1-N} + \frac{f_{\rm DM2}}{M_{\rm DM2}}\,\sigma^{\rm SI}_{\rm DM2-N}$$

- A large parameter space is available in our model that eludes experimental bounds including DD constraints and satisfies PLANCK measured relic limits.
- For, Indirect Detection, both fermion and triplet DM are insensitive to the current limits.

Phase Transition Dynamics

- Dynamic fields $\dashrightarrow$ $h,\ s,\ T^0$

$$V_{\text{eff}}^T = V_{\text{tree}} + \Delta V + V'^{\text{1-loop}}_{\text{CW}} + V^{\text{1-loop}}_{T\neq 0} + V_{\text{ct}}$$

- V_{tree} in terms of dynamic fields,

$$V_{\text{tree}} = -\frac{\mu_H}{2}h^2 - \frac{\mu_S}{2}s^2 - \frac{\mu_T}{2}T^{0\,2} + \frac{\lambda_H}{4}h^2 + \frac{\mu_{HS}}{2}h^2 s + \frac{\lambda_{HS}}{4}h^2 s^2 - \frac{\mu_3}{3}s^3 + \frac{\lambda_s}{4}s^4$$
$$+\frac{\lambda_{HT}}{2}h^2 T^{0\,2} + \frac{\lambda_{ST}}{2}s^2 T^{0\,2} + \frac{\lambda_T}{4!}T^{0\,4}$$

- Different possible PT patterns,

"one-step"

$\mathcal{O} \to \mathcal{H}$

$\mathcal{O} \to \mathcal{S}$

$\mathcal{S} \to \mathcal{SH}$

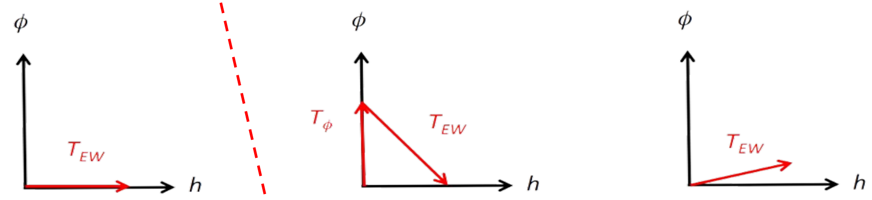

- Also along the Triplet direction at high temp. in some region. However, at zero temp. it must be 0.
- We are not interested any transition along the triplet.

Presence of such couplings are crucial as they give rise to potential barrier along h(s)-direction at the tree-level itself!

PT Dynamics Results

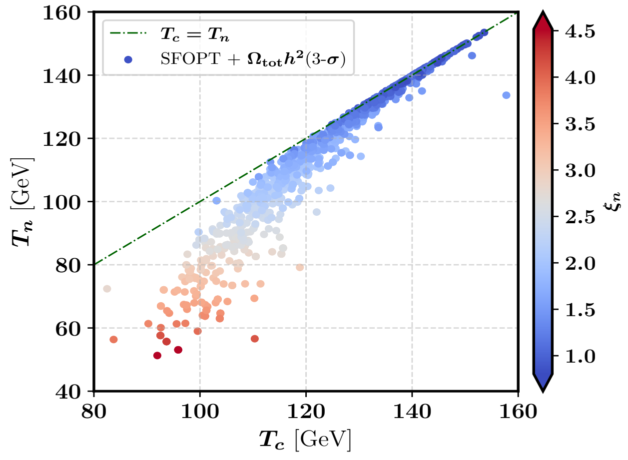

SFOPT: 1. $\xi_c = \frac{v_c}{T_c} \gtrsim 1.0$

2. $\xi_n = \frac{\sqrt{(h_{\rm lT} - h_{\rm hT})^2}}{T_n} \gtrsim 1.0$

Characteristics temperatures

- Critical temp. (T_c)
- Nucleation temp. (T_n)
- Percolation temp. (T_p)

A recommended "reference" temp.
To evaluate thermal parameters determining GWs.

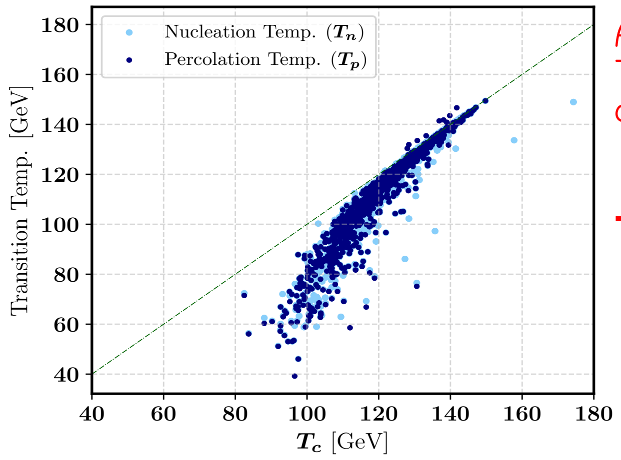

➔ T_p is not much deviated from T_n except in transitions with lower temperatutes.

Tree-level contribution

1-loop, T=0

1-loop, thermal

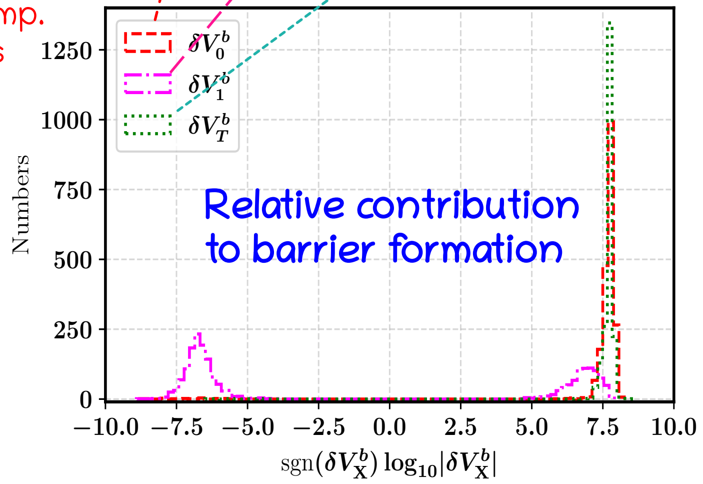

PT Dynamics Results

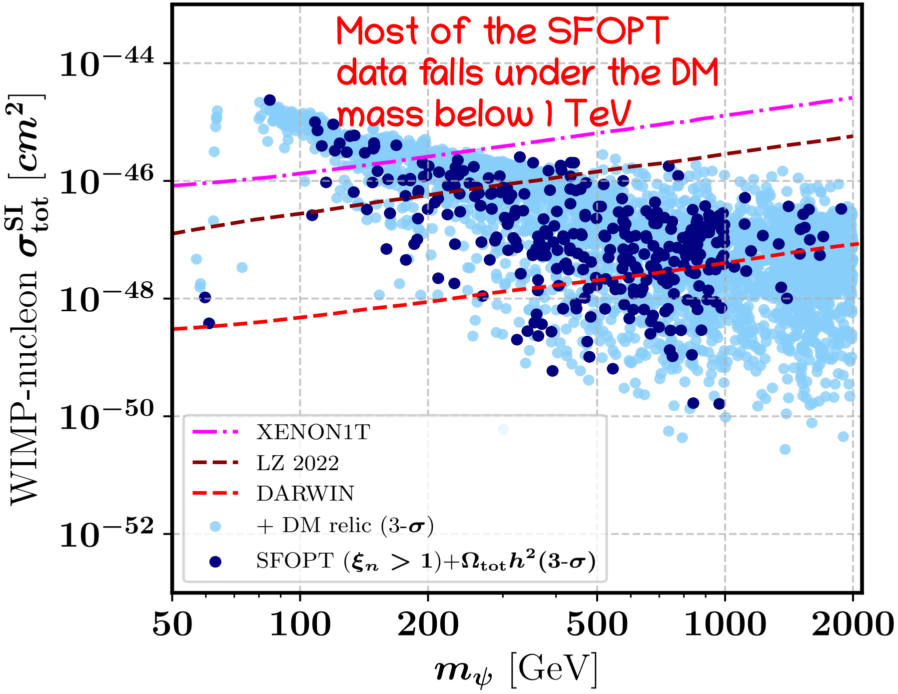

- Apart from the DM masses, the phenomenology of the multi-DM is, mostly, determined by g_S and $\sin\theta$
- On the other hand, additional scalar couplings $\mu_{HS}(\lambda_S)$ and μ_3 aid in generating a SFOPT, which doesn't impact the DM phenomenology significantly.
- The above feat is usually absent in a typical **"ITM+real scalar"** extension with $\mathcal{Z}_2$ symmetry.
- Moreover, the constraint on $\sin\theta$ from the demand of a SFOPT is also relaxed in our setup.

PT parameters and GW spectra

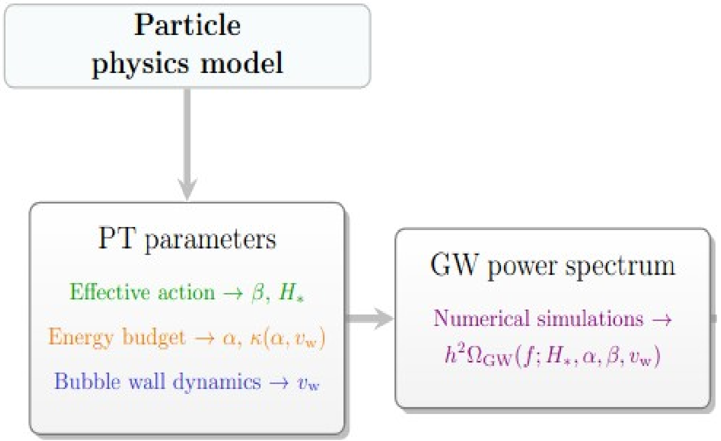

- α and β/H_* depends on your particle physics model,

$\alpha = \frac{\Delta\rho}{\rho_{rad}}$, latent heat released by the PT process

$$\rho_{rad} = \frac{g^* \pi^2}{30} T_*^2$$

$$\Delta\rho = \left[V_{\rm eff}^T(\phi_0, T) - T\frac{dV_{\rm eff}^T(\phi_0,T)}{dT}\right]_{T=T_*} - \left[V_{\rm eff}^T(\phi_n, T) - T\frac{dV_{\rm eff}^T(\phi_n,T)}{dT}\right]_{T=T_*}$$

$\frac{\beta}{H_*} = \left[T.\frac{d(S_E/T)}{dT}\right]_{T=T_*}$, $v_w \longrightarrow 1$ (a conservative choice)

GWs: production

Bubble collisions: $\Omega_{\rm col} h^2$

Kosowsky, Turner, Watkins, PRL 69 (1992) 2026; PRD 45 (1992) 4514; Weir, PRD 93 (2016) 124037; Huber, Konstandin, JCAP 0809 (2008) 022; Cutting, Hindmarsh, Weir, PRD 97 (2018) 123513, etc.

In general negligible, except for very strong super cooling.

In most cases, such amount of supercooling incompatible with PT completion... *Ellis, Lewicki, No, JCAP 1904 (2019) 003*

A few exception, e.g., conformal scalar potentials

Sound waves: $\Omega_{\rm sw} h^2$

Hindmarsh, Huber, Rummukainen, Weir, PRL 112 (2014) 041301; PRD 92 (2015) 123009; PRD 96 (2017) 103520; Konstandin, JCAP 1803 (2018) 047; Hindmarsh, Hijazi, arXiv:1909.10040

Typically dominant signal.

Works for low bubble velocity!

$$h^2\Omega_{\rm sw}(f) = 2.59\times 10^{-6} \underbrace{\left(\frac{g_*}{100}\right)^{-\frac{1}{3}}}_{\textit{Redshift}} \underbrace{\left(\frac{\kappa_{\rm sw}\alpha}{1+\alpha}\right)^2 \left(\frac{\max(v_w, c_{s,f})}{c}\right)\left(\frac{\beta}{H_*}\right)^{-1}\Upsilon(\tau_{\rm sw})}_{\textit{Scaling}} \underbrace{S_{\rm sw}(f)}_{\textit{Shape}},$$

$$f_{\rm sw} = 8.9\times 10^{-6}\,{\rm Hz} \underbrace{\left(\frac{g_*}{100}\right)^{\frac{1}{6}}\left(\frac{T_*}{100\,{\rm GeV}}\right)}_{\textit{Redshift}} \underbrace{\left(\frac{c}{\max(v_w, c_{s,f})}\right)\left(\frac{\beta}{H_*}\right)\left(\frac{z_p}{10}\right)}_{\textit{Scaling}},$$

$$\Upsilon(\tau_{\rm sw}) = 1 - \frac{1}{\sqrt{1+2\tau_{\rm sw}H_*}},\quad S_{\rm w}(f) = \left(\frac{f}{f_{\rm sw}}\right)^3\left[\frac{7}{4+3(f/f_{\rm sw})^2}\right]^{7/2}$$

Turbulence: $\Omega_{\rm turb} h^2$

Numerical simulations are going on! Semi-analytic approximations exists so far.

GW spectra

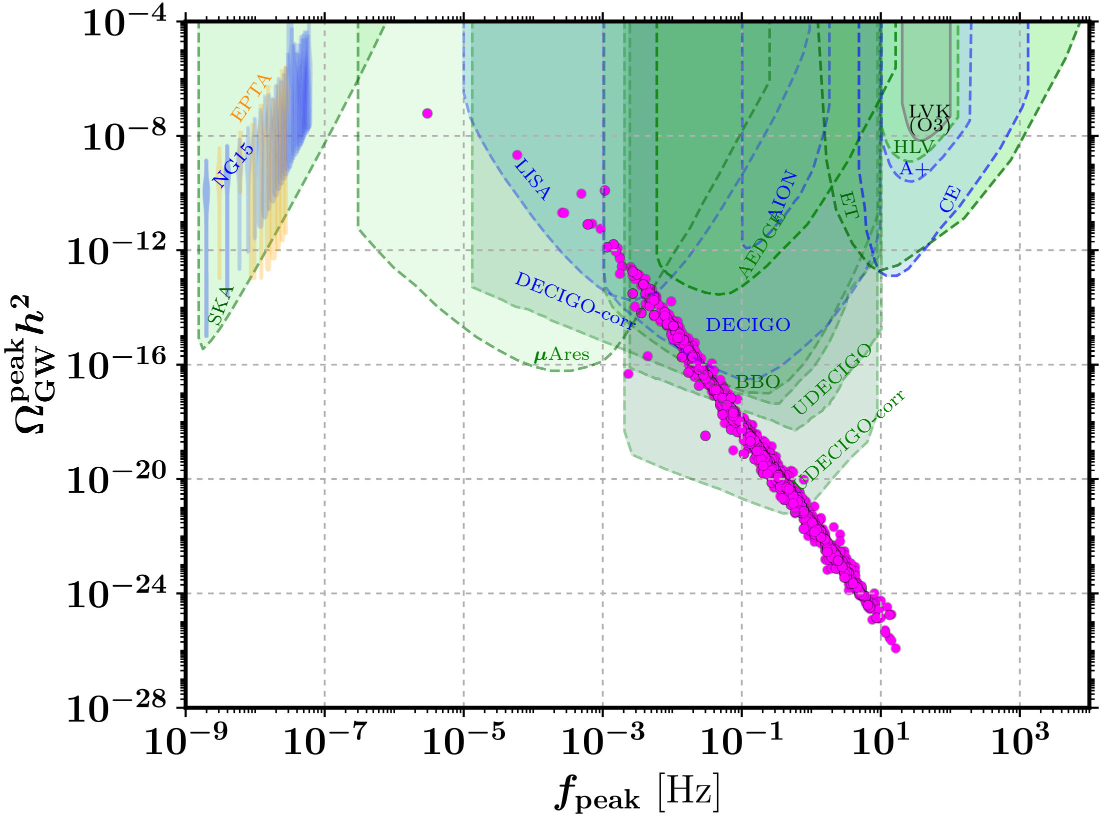

$\Omega_{\rm GW}^{\rm peak} h^2$
$f_{\rm peak}$ [Hz]
EPTA
NG15
SKA
LISA
DECIGO-corr
μAres
DECIGO
BBO
AEDGE
AION
ET
UDECIGO
UDECIGO-corr
LVK
(O3)
HLV
A+
CE

GW detectablity-I

Conventional strategy:

- Obtain the peak frequency and peak amplitudes and project them against experimental sensitivity limits of respective GW detectors.

- Calculate sound-to-noise (SNR) w.r.t GW detectors and check its detectability against respective Project them against experimental sensitivity limits of respective GW detectors **power-law-integrated sensitivity curves (PLIs).** *E. Thrane and J. D. Romano Phys. Rev. D 88 (2013)*

$$\mathrm{SNR} \equiv \sqrt{T}\left[\int_{f_{\rm min}}^{f_{\rm max}} \left(\frac{\Omega_{\rm signal}(f)}{\Omega_{\rm noise}(f)}\right)^2 df\right]^{1/2}$$

Time duration of mission, generally, 4 years.

Detector noise data.

Amplitude obtained for a particular physics model with a given parameter set.

GW detectablity: PLIs

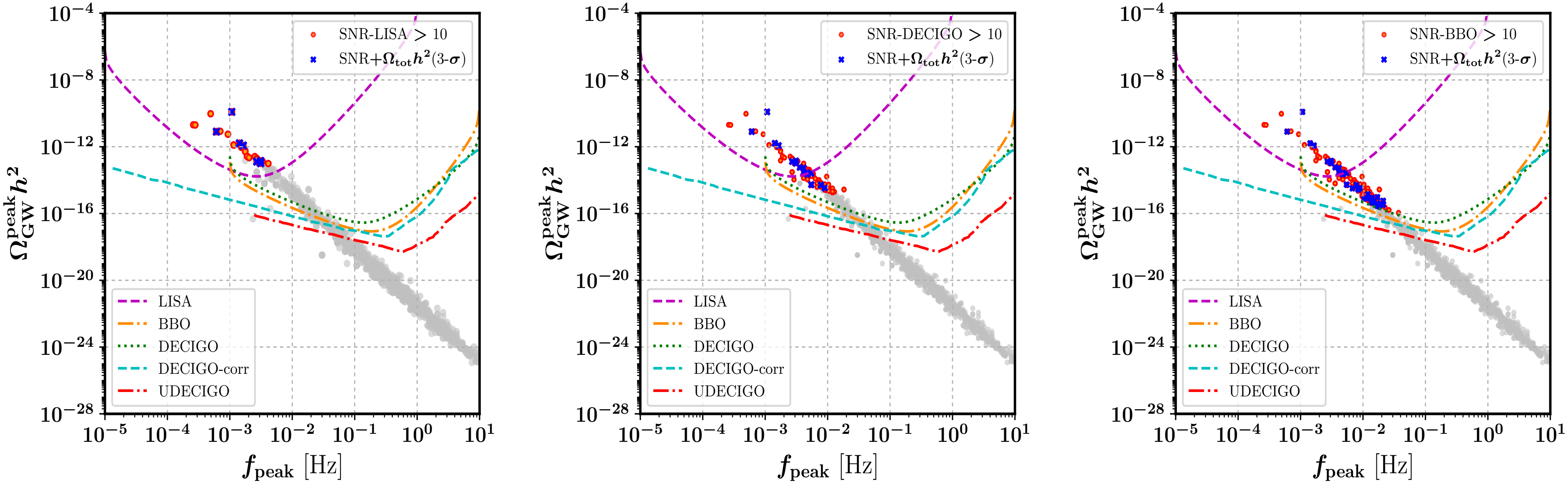

We obtain parameter points with SNR > 10 that satisfies DM relic + DD constraints and they can be detected in LISA, BBO, DECIGO.

GW detectablity-II

Limitations of PLIs:

- Calculation of peak freq. and peak amp. of individual points carries no inherent information about SNR.
- Note that, PLIs only have a well defined satistical meaning for GW signals that are described by a power law, which is maximally violated close to the “peak” in the GW spectrum due to SFOPT.

T. Alane et. al., JHEP 03 (2020) 004; K. Schmitz, JHEP 01 (2021) 097

Another approach: Peak Integrated Sensitivity Curves (PISCs)

$$\rho = \left[n_{\rm det} \frac{t_{\rm obs}}{s} \int_{f_{\rm min}}^{f_{\rm max}} \left(\frac{\Omega_{\rm signal}(f)}{\Omega_{\rm noise}(f)} \right)^2 df \right]^{1/2} \longleftrightarrow \frac{\rho^2}{t_{\rm obs}/{\rm yr}} = \left(\frac{h^2\Omega_{\rm b}^{\rm peak}}{h^2\Omega_{\rm PIS}^{\rm b}}\right)^2 + \left(\frac{h^2\Omega_{\rm sw}^{\rm peak}}{h^2\Omega_{\rm PIS}^{\rm sw}}\right)^2 + \left(\frac{h^2\Omega_{\rm t}^{\rm peak}}{h^2\Omega_{\rm PIS}^{\rm t}}\right)^2 + \left(\frac{h^2\Omega_{\rm b/sw}^{\rm peak}}{h^2\Omega_{\rm PIS}^{\rm b/sw}}\right)^2 + \left(\frac{h^2\Omega_{\rm sw/t}^{\rm peak}}{h^2\Omega_{\rm PIS}^{\rm sw/t}}\right)^2 + \left(\frac{h^2\Omega_{\rm b/t}^{\rm peak}}{h^2\Omega_{\rm PIS}^{\rm b/t}}\right)^2 .$$

Auto or cross-correlation measurement

$$h^2\Omega_{\rm PIS}^{i/j} \equiv \left[(2-\delta_{ij})\, n_{\rm det}\, 1\,{\rm yr} \int_{f_{\rm min}}^{f_{\rm max}} {\rm d}f\, \frac{S_i(f)\, S_j(f)}{(h^2\Omega_{\rm noise}(f))^2} \right]^{-1/2}$$

$$h^2\Omega_{i/j}^{\rm peak} = \left(h^2\Omega_i^{\rm peak}\, h^2\Omega_j^{\rm peak} \right)^{1/2} .$$

$i, j \in \{{\rm b}, {\rm sw}, {\rm t}\}$

GW detectablity: PISCs

Advantages of PISCs:

- PISCs are constructed in a way such that they retain full information on the SNR.
- For a given experiment and observation time, the SNR is uniquely determined by the peak energy densities and the corresponding peak frequencies, once the “mother integral” is carried out.
- A given point in the PISc plot, the SNR correspond to the vertical separation between the point & PISC of interest. Think of DD limits & exclusion as an analogy!

$$\rho = \left[n_{\rm det}\,\frac{t_{\rm obs}}{s}\int_{f_{\rm min}}^{f_{\rm max}}\left(\frac{\Omega_{\rm signal}(f)}{\Omega_{\rm noise}(f)}\right)^2 df\right]^{1/2} \Longleftrightarrow \frac{\rho^2}{t_{\rm obs}/{\rm yr}} = \left(\frac{h^2\Omega_{\rm b}^{\rm peak}}{h^2\Omega_{\rm PIS}^{\rm b}}\right)^2 + \left(\frac{h^2\Omega_{\rm sw}^{\rm peak}}{h^2\Omega_{\rm PIS}^{\rm sw}}\right)^2 + \left(\frac{h^2\Omega_{\rm t}^{\rm peak}}{h^2\Omega_{\rm PIS}^{\rm t}}\right)^2 + \left(\frac{h^2\Omega_{\rm b/sw}^{\rm peak}}{h^2\Omega_{\rm PIS}^{\rm b/sw}}\right)^2 + \left(\frac{h^2\Omega_{\rm sw/t}^{\rm peak}}{h^2\Omega_{\rm PIS}^{\rm sw/t}}\right)^2 + \left(\frac{h^2\Omega_{\rm b/t}^{\rm peak}}{h^2\Omega_{\rm PIS}^{\rm b/t}}\right)^2 .$$

Mother Integral!

$$h^2\Omega_{\rm PIS}^{i/j} \equiv \left[(2-\delta_{ij})\,n_{\rm det}\,1\,{\rm yr}\int_{f_{\rm min}}^{f_{\rm max}} {\rm d}f\,\frac{S_i(f)\,S_j(f)}{\left(h^2\Omega_{\rm noise}(f)\right)^2}\right]^{-1/2} \qquad h^2\Omega_{i/j}^{\rm peak} = \left(h^2\Omega_i^{\rm peak}\,h^2\Omega_j^{\rm peak}\right)^{1/2} .$$

$i, j \in \{{\rm b}, {\rm sw}, {\rm t}\}$

GW detectablity: PISCs

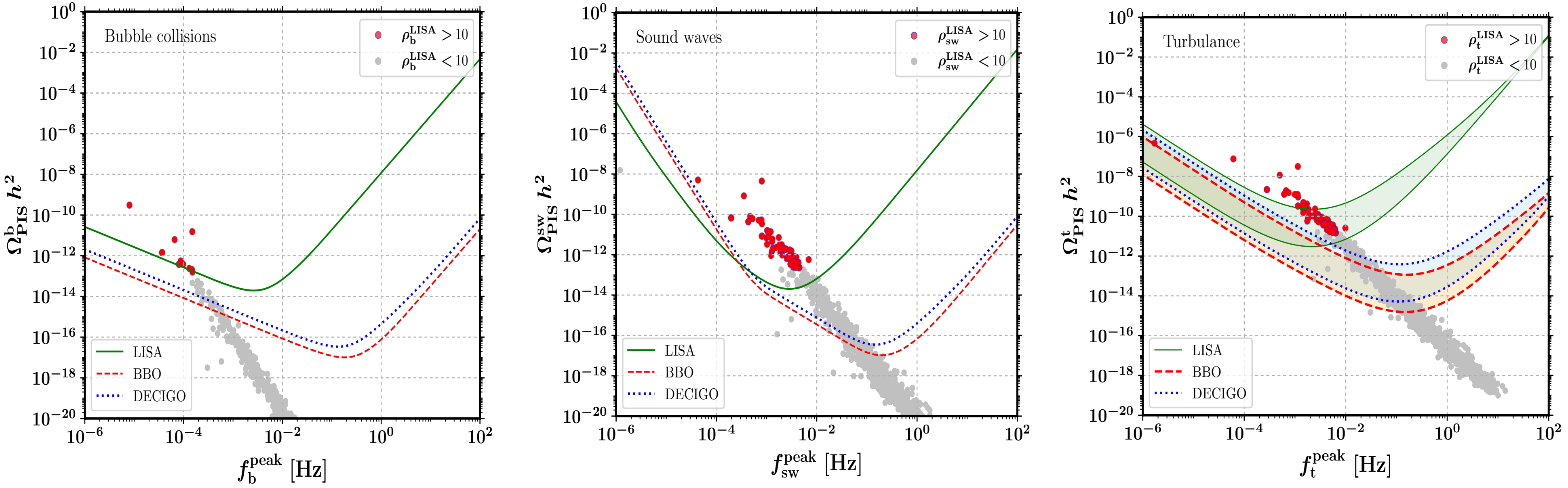

- Fig. shows analysis for LISA only with observation time 4 years. Can be extended for other detectors.
- Read the plots as, any data points that falls on or above any experimental curves are allowed by their respective SNR.
- Points that are below the curve needs inspection individually for different detectors.

GW detectablity: PISCs

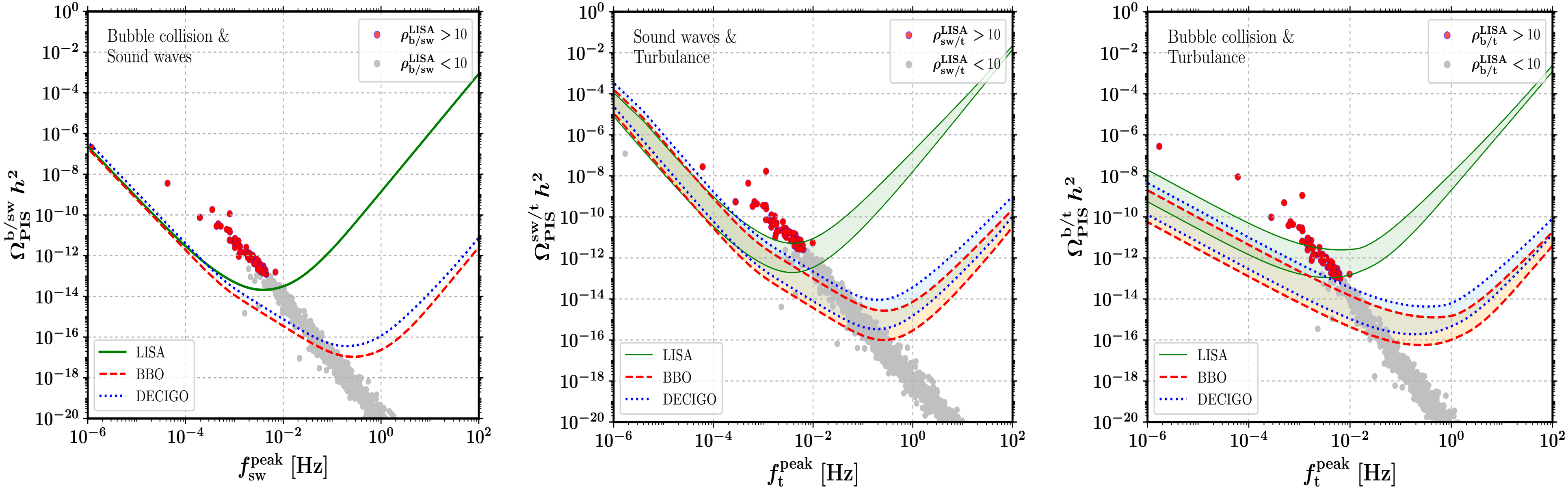

Plots with cross-correlations of different GW sources due to SFOPT.

Conclusion & Summary

- We successfully revived the “desert” region for the triplet dark matter in the interested region, i.e., [300, 1000] GeV. Moreover, a wide range for the fermionic dark matter is allowed from around $m_{h_2}/2$ to over the TeV scale leaving a large parameter region for rich phenomenology.

- We further estimate the gravitational wave signals (GW) arising from such SFOPT by comparing them with the **power-law-integrated sensitivity limits (PLIs)** and also with the **peak-integrated sensitivity curves (PISCs)** to examine the detectibility prospects.

- **We find parameter points that evades experimental constraints, satisfies DM relic and DD limits and also lie within the detectable sensitivity range of LISA, BBO, DECIGO etc**.

- Our investigation complements the collider searches of BSM new physics at the DM and GW detector frontiers.

Back-Up Slides

Constraints on the model

I. Theoretical Constraints

- Perturbativity
- Vacuum stability (bounded-from-below)
- Perturbative unitarity
- Electroweak precision test (oblique parameters)

II. Experimental Constraints

- SM Higgs searches (e.g., diphoton decay, etc.)
- BSM Higgs searches and other collider limits
- DM relic density
- DM direct & indirect detection

III. PT Constraints

- Correct EW vacuum at T=0
- Successfull nucleation & percolation criterion
- . . .

- We used **FeynRules**, **micrOMEGAs**, **HiggsBounds, HiggsSignals/Lilith** and personal python codes to check contraints I. & II
- **CosmoTransitions** is utilized to implement **PT analysis** and to obtain **GW** observables

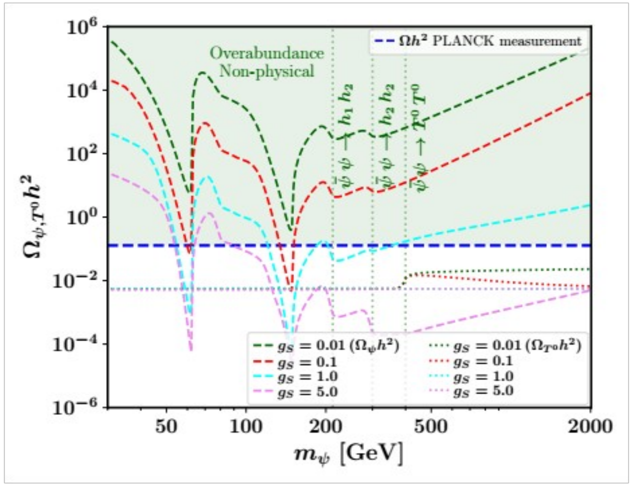

(a)

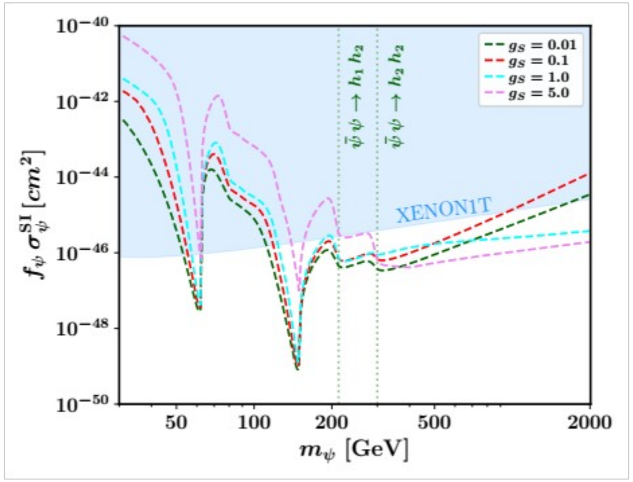

(b)

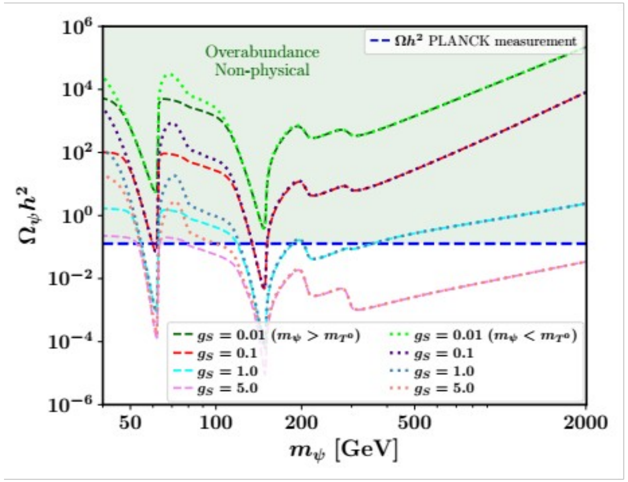

(c)

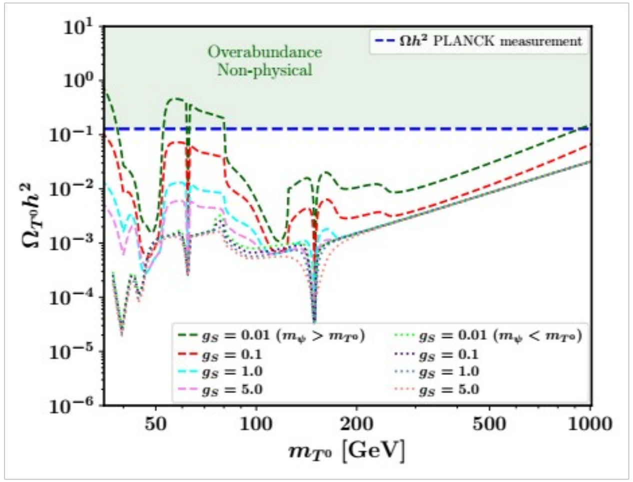

(d)

Some dependence
on model parameters

General Scan and Results

- **For the general scan, we choose the parameters as,**

Parameter	Range
m_S	$[130, 2000]$
m_{T^0}	$[300, 1000]$
m_ψ	$[10, 2000]$
v_S	$[-1000, 1000]$
μ_3	$[-1000, 1000]$
μ_{ST}	$[-1000, 1000]$
θ	$[-0.2, 0.2]$
λ_S	$[0.001, 3.5]$
g_S	$[0.01, 3.5]$
λ_{ST}	$[0.01, 0.3]$
λ_{HT}	$[0.01, 0.3]$

Lower limit appears from collider constraints, and we want it to be in the "desert region" and hence the upper limit

This range is inspired from EWPT point of view as it demands parameters to be at (or near to) EW scale

Conservative limit due to BSM Higgs searches, EWPO and W-boson mass.

Inspired from previous findings and perturbativity

- **We fix $\lambda_T = 0.05$ throughout**

First-order EW Phase Transition

- The main ingredient to investigate the phase transition is the effective potential, in general,

$$\boxed{V_{\rm eff}^T = V_{\rm tree} + \Delta V + {V'}_{\rm CW}^{1-{\rm loop}} + V_{T\neq 0}^{1-{\rm loop}} + V_{\rm ct}}$$

$V_{\rm tree}$ is the tree level potential of the underlying theory.

$${V'}_{\rm CW}^{1-{\rm loop}} = \frac{1}{64\pi^2}\sum_{i=B,F}(-1)^{F_i} n_i m_i^4(\phi_\alpha, T)\left[\log\left(\frac{m_i^2(\phi_\alpha,T)}{\Lambda^2}\right) - \mathcal{C}_i\right]$$

$m_i^2(\phi_\alpha, T) = m_i^2(\phi_\alpha) + c_i T^2$, $c_i \to$ Daisy coefficients.

c_i can be calculated using the high-temperature limit with $\frac{1}{T^2}\frac{\partial^2 V_{T\neq 0}^{1-{\rm loop}}}{\partial\phi_i\partial\phi_j}$

$$V_{T\neq 0}^{1-{\rm loop}} = \frac{T^4}{2\pi^2}\sum_{i=B,F}(-1)^{F_i} n_i J_{B/F}\left(\frac{m_i^2(\phi_\alpha,T)}{T^2}\right)$$

$$J_{B/F}\left(x^2 \equiv \frac{m_i^2(\phi_\alpha,T)}{T^2}\right) = \pm\int_0^\infty dy\; y^2 \log\left(1 \mp e^{-\sqrt{x^2+y^2}}\right)$$

V_{ct} = counter term potential

$$\frac{\partial}{\partial\phi_i}\left(V_{\rm eff} + V_{\rm ct}\right)\Big|_{\phi_i=\langle\phi_i\rangle} = 0 \quad \text{and} \quad \frac{\partial^2}{\partial\phi_i\partial\phi_j}\left(V_{\rm eff} + V_{\rm ct}\right)\Big|_{\phi_i=\langle\phi_j\rangle} = 0,$$

GW analysis

- Generally, bubble velocity is either calculated by solving hydrodynamic equations or consider it as **input** parameter.
- However, in some approximation, analytic form of v_w is also available.
- We calculate v_w analytically for points with SFOPT and identify **different regions** for bubble's motion in plasma.

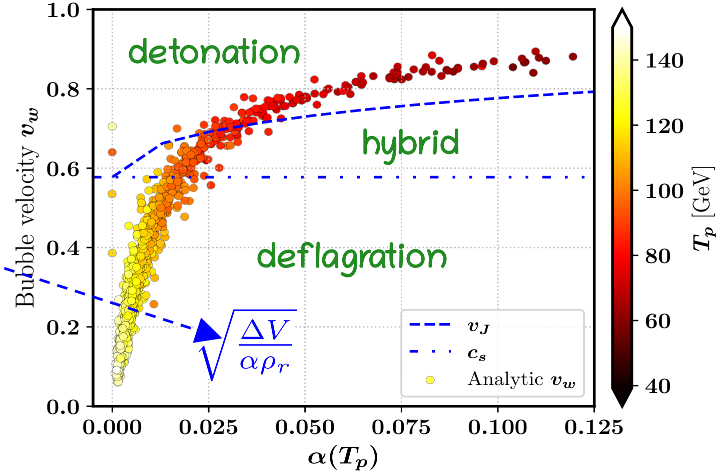

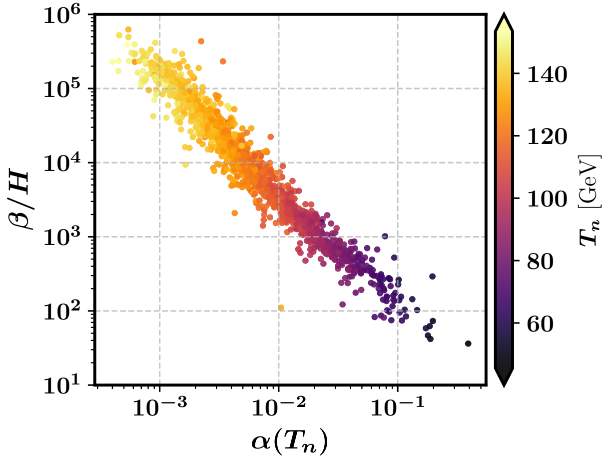

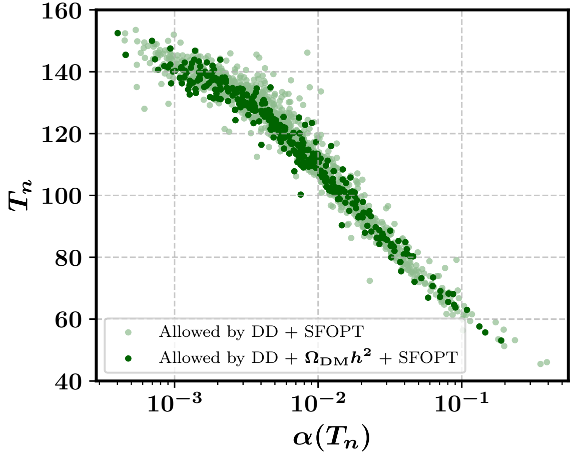

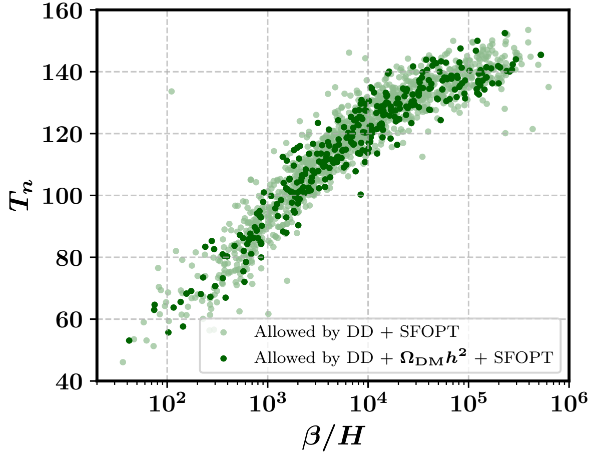

Spectral shapes:

$$S_{\rm b}(f, f_{\rm b}) = \frac{3.8\,(f/f_{\rm b})^{2.8}}{1+2.8\,(f/f_{\rm b})^{3.8}}\,,$$

$$S_{\rm s}(f, f_{\rm s}) = \frac{(f/f_{\rm s})^{3}}{[4/7+3/7\,(f/f_{\rm s})^{2}]^{\frac{7}{2}}}\,,$$

$$S_{\rm t}(f, f_{\rm t}, h_*) = \frac{(f/f_{\rm t})^{3}}{(1+8\pi f/h_*)[1+(f/f_{\rm t})]^{\frac{11}{3}}}\,.$$

$$h_*(T_*) = \frac{a_*}{a_0}\,H_*(T_*) = 1.6\cdot 10^{-5}\,{\rm Hz}\left(\frac{g_*(T_*)}{100}\right)^{\frac{1}{6}}\left(\frac{T_*}{100\,{\rm GeV}}\right)$$